JOURNAL OF CELLULAR PHYSIOLOGY 196:493–503 (2003)

Ionic Basis for Excitability of Normal Rat Kidney (NRK) Fibroblasts

E.G.A. HARKS,[1] J.J. TORRES,[2,3] L.N. CORNELISSE,[3,4] D.L. YPEY,[1,5] AND A.P.R. THEUVENET[1]*

[1]*Department of Cell Biology, University of Nijmegen, Nijmegen, The Netherlands*
[2]*Institute "Carlos I" for Theoretical and Computational Physics and Department of Electromagnetism and Material Physics, University of Granada, Granada, Spain*
[3]*Department of Medical Physics and Biophysics, University of Nijmegen, Nijmegen, The Netherlands*
[4]*Department of Cellular Animal Physiology, University of Nijmegen, Nijmegen, The Netherlands*
[5]*Department of Physiology, Leiden University Medical Center, Leiden, The Netherlands*

Ionic membrane conductances of normal rat kidney (NRK) fibroblasts were characterized by whole-cell voltage-clamp experiments on single cells and small cell clusters and their role in action potential firing in these cells and in monolayers was studied in current-clamp experiments. Activation of an L-type calcium conductance (G_{CaL}) is responsible for the initiation of an action potential, a calcium-activated chloride conductance ($G_{Cl(Ca)}$) determines the plateau phase of the action potential, and an inwardly rectifying potassium conductance (G_{Kir}) is important for the generation of a resting potential of approximately −70 mV and contributes to action potential depolarization and repolarization. The unique property of the excitability mechanism is that it not only includes voltage-activated conductances (G_{CaL}, G_{Kir}) but that the intracellular calcium dynamics is also an essential part of it (via $G_{Cl(Ca)}$). Excitability was found to be an intrinsic property of a fraction (∼25%) of the individual cells, and not necessarily dependent on gap junctional coupling of the cells in a monolayer. Electrical coupling of a patched cell to neighbor cells in a small cluster improved the excitability because all small clusters were excitable. Furthermore, cells coupled in a confluent monolayer produced broader action potentials. Thus, electrical coupling in NRK cells does not merely serve passive conduction of stereotyped action potentials, but also seems to play a role in shaping the action potential. J. Cell. Physiol. 196: 493–503, 2003. © 2003 Wiley-Liss, Inc.

Fibroblasts constitute the connective tissues of the body and are generally considered to be classical examples of non-excitable cells. For maintaining the integrity of the organ and tissue structure, fibroblasts are in continuous chemical communication with other surrounding cells via the intercellular space, while they are in direct contact with each other through intercellular channels organized in specialized contact structures called gap junctions. In a large number of studies, we have used normal rat kidney (NRK) fibroblasts as an in vitro model system to study the mechanism(s) of growth regulation of cells by polypeptide growth factors (van Zoelen, 1991; Lahaye et al., 1999).

Previous studies have shown that confluent monolayers of NRK cells that have been made quiescent in their proliferation by removal of growth factors from their culture medium (further referred to as quiescent cells) have a stable resting membrane potential around −70 mV (De Roos et al., 1997a). Under these conditions, the cells in the monolayer are electrically well coupled by gap junctions (De Roos et al., 1996; Harks et al., 2001). Remarkably, because these cells are usually considered as non-excitable cells, a propagating action potential can be induced in these monolayers by depolarizing cells in a small area in the monolayer. This depolarization can be achieved by either a local application of increased extracellular $[K^+]$ or of an intracellular calcium-mobilizing agent (e.g., bradykinin). In this way, a single action potential is evoked characterized by a fast

Contract grant sponsor: The Spanish Ministerio de Ciencia y Technologia and FEDER ("Ramón y Cajal"); Contract grant number: BFM2001-2841; Contract grant sponsor: University of Granada (Plan Propio de Investigación); Contract grant sponsor: The Dutch Foundation for Neural Networks (SNN); Contract grant sponsor: Foundation Nijmegen University Fund (SNUF).

*Correspondence to: Alexander P.R. Theuvenet, Department of Cell Biology, Toernooiveld 1, 6525 ED Nijmegen, The Netherlands. E-mail: ATheuv@sci.kun.nl

Received 8 August 2002; Accepted 14 March 2003

DOI: 10.1002/jcp.10346

depolarizing spike to positive membrane potentials followed by a plateau phase around −20 mV that lasts about 30 sec. These action potentials have been shown to propagate through the entire monolayer with a velocity of approximately 1 cm/sec and are accompanied by an almost synchronized transient increase in the cytoplasmic Ca^{2+} concentration in all the cells in the monolayer (De Roos et al., 1997b). Apparently, like excitable cells such as cardiomyocytes and neuronal cells, NRK fibroblasts are able to communicate over a long distance by electrical signaling. The in vivo function of this excitability, however, is still unknown.

In the present study, we performed whole-cell voltage-clamp experiments to identify and characterize the membrane conductances of major importance for NRK cell excitability. We show for the first time, that in addition to an L-type calcium conductance and a calcium-activated chloride conductance (De Roos et al., 1997a,c), NRK cells possess a prominent inwardly rectifying potassium conductance, and that the action potential evoked in cells and monolayers results from a sequential activation of each of these three conductances. We also show that excitability is not restricted to electrically coupled cells in monolayer culture, because a significant percentage of single isolated cells was already able to generate action potentials.

MATERIALS AND METHODS

Cell culturing

NRK fibroblasts (NRK clone 49F) were cultured in bicarbonate buffered Dulbecco's modified Eagle's medium (DMEM; Life Technologies, Paisly, UK) supplemented with 10% newborn calf serum (HyClone Laboratories, Logan, UT) and confluent cultures were made quiescent by a subsequent 1–3 days incubation in serum-free DF medium (DMEM/Ham's F12, 1:1; Gibco, Life Technologies Breda, The Netherlands) supplemented with 30 nM Na_2SeO_3 and 10 μg/ml human transferrin. For the experiments on single cells and cell clusters, cells were dissociated from quiescent monolayers by addition of a 0.25% trypsin solution for 5 min, after which cells were seeded in serum-free DF medium. The experiments on the dissociated cell cultures were performed 2–4 h after trypsinization when NRK cells had been sufficiently attached to the culture dish.

Electrophysiology

Patch-clamp experiments were performed at room temperature on single cells, small cell clusters (≤10 cells), and monolayers. The cells were perfused with a standard extracellular solution, DF-ECS, which was the DF medium (DMEM/Ham's F12, 1:1; Gibco, Life Technologies) containing (in mM) 120 NaCl, 4.2 KCl, 2 $CaCl_2$, 0.3 $MgCl_2$, 0.4 $MgSO_4$, 44 $NaHCO_3$, and 1.0 NaH_2PO_4, equilibrated with 7.5% CO_2 to pH 7.4. Data were obtained using an EPC-7 patch-clamp amplifier (List Electronic, Darmstadt, Germany) in conjunction with Pulse/Pulsefit software (HEKA Elektronik, Lambrecht, Germany). The electrode was inserted in a side pool filled with the pipette solution and connected to the bath solution via a salt bridge with bath solution. For whole-cell voltage-clamp measurements on cells and clusters of two to ten cells data were sampled at 10 kHz and the fast capacitive current transients were cancelled at the beginning of each experiment. In the current-clamp experiments on single cells and cell clusters, the resting membrane potential was preset to −80 mV by a holding current. The standard intracellular pipette solution (S-ICS) contained (in mM) 25 NaCl, 120 KCl, 1 $CaCl_2$, 1 $MgCl_2$, 3.5 EGTA, 10 HEPES/KOH (pH 7.4), which corresponds to a free calcium concentration of ∼55 nM (Schoenmakers et al., 1992). Pipettes with a resistance of 4–6 MΩ were used for optimal whole-cell stability. Series resistances were approximately <15 MΩ, causing acceptable voltage errors <3 mV at small currents (<200 pA) in the single cell whole-cell voltage-clamp experiments. For the characterization of the L-type current, clusters of five to seven cells that had been dissociated from quiescent monolayers were used. In these experiments, the extracellular solution (Sr-ECS) consisted of (in mM) 130 TEACl, 2 $SrCl_2$, 1 $MgCl_2$, 10 glucose, and 10 HEPES, pH 7.4 supplemented with 50 μM NPPB, while pipettes were filled with Cs-ICS, composed of 145 CsCl, 1 $MgCl_2$, 4 MgATP, 3.5 EGTA, and 10 HEPES, pH 7.4.

Estimation of maximal conductances

Ionic membrane conductances in single cells were calculated from current–voltage relationships (I–V curves). The leak conductance (G_{leak}) was calculated by dividing the total current at −80 mV by the driving force for the leak current (−80 mV), assuming $E_{leak} = 0$ mV. At a potential of −80 mV, which is the approximate equilibrium potential for potassium, only the leak contributes to the total current. In the voltage range measured, the inwardly rectifying potassium conductance (G_{Kir}) was maximal at −120 mV. Therefore, the maximal conductance was calculated at that potential by dividing the maximal total current after leak correction, by the driving force for potassium (−40 mV). The inward calcium current was maximal at 0 mV, but because the L-type calcium conductance (G_{CaL}) was larger around its reversal potential ($+46.8 \pm 1.8$ mV, $n = 36$), it was calculated by determining the slope of the I–V curve at that potential. Finally, the calcium-activated chloride conductance ($G_{Cl(Ca)}$) was estimated by dividing the leak-corrected maximal outward current at +40 mV by the driving force for chloride at this potential in cells in which the calcium-activated chloride current was maximized by minimal intracellular calcium buffering. Current-clamp experiments on NRK monolayers have shown before that the equilibrium potential for chloride in monolayers is about −20 mV for these cells (De Roos et al., 1997a), but in our single-cell and cell cluster whole-cells, we expect $E_{Cl} \sim 0$ mV because of the applied symmetrical chloride concentration. Therefore, the driving force for chloride at +40 mV was assumed to be 40 mV. Membrane conductances in cell clusters were determined in the same way and were normalized as conductances per cluster cell by dividing the total membrane conductance by the number of cells. The calculated maximal conductances in cell clusters are underestimates. The error in the conductance estimation first depends on the size of the current and the value of the total series resistance to the surrounding cells. Series resistance to the

membrane of the patched cell was <15 MΩ and the gap junctional resistance from the patched cell to the surrounding cells <10 MΩ (Harks et al., 2001), thus total series resistance was <25 MΩ. For currents <200 pA, this results in a <5 mV voltage error, which is approximately <12.5% error in an applied driving force of 40 mV (for G_{Kir} and $G_{Cl(Ca)}$). The underestimation of the conductance is of course larger, because of the voltage-activated properties of G_{Kir} and $G_{Cl(Ca)}$. For G_{Kir}, we estimated a rough conductance error of ~20% based on non-linear I–V's for small total currents as in Figure 1D. However, these values are approximations, merely serving to make sure that the better estimations are obtained from the smaller currents, for example, the L-type calcium currents, which can better be resolved in the clusters. These currents were <50 pA, when measured in clusters in the presence of NPPB, thus the calculated voltage-clamp error in these experiments was <1.25 mV, which may be considered as acceptable. Maximal conductances in single cells and clusters were compared with a Mann–Whitney *U*-test and the correlation between the duration of the action potential and the (relative) size of the maximal conductances was determined with a Spearman's Rho test. Data are represented as mean ± SEM for n cells throughout this article.

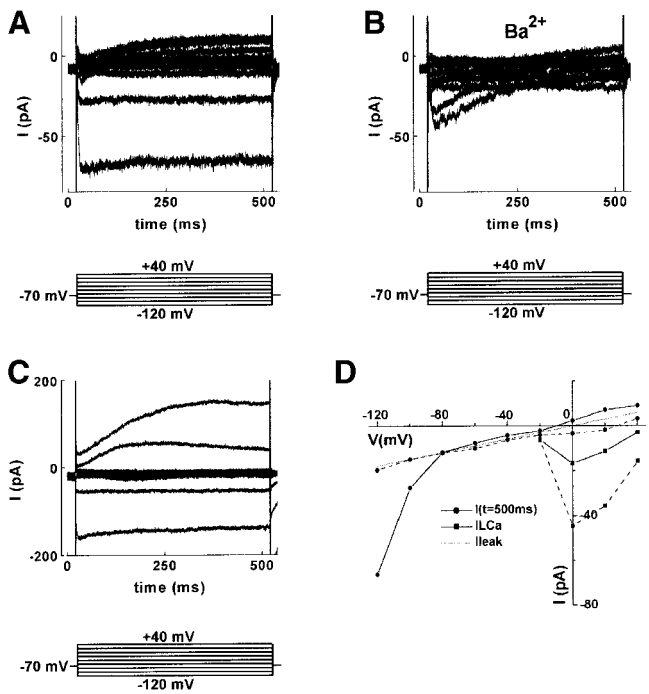

Fig. 1. Whole-cell current records and current–voltage relationships (I–V curves) in single cells. **A**: Single cell (21.0 pF) with an inwardly rectifying potassium conductance ($G_{Kir,max}$ = 1.34 nS), an L-type calcium conductance ($G_{CaL,max}$ = 0.68 nS), and a calcium-activated chloride conductance ($G_{Cl(Ca),max}$ = 0.08 nS). **B**: Same cell in the presence of 5 mM external Ba^{2+}. **C**: Single cell (20.8 pF) measured with weakly buffering pipette solution containing 100 μM EGTA and 0 mM $CaCl_2$, $G_{Kir,max}$ = 3.44 nS, $G_{CaL,max}$ = 0.52 nS, and $G_{Cl(Ca),max}$ = 4.35 nS. In all experiments, voltage-clamp steps were applied from a holding potential (Vh) of −70 mV to test potentials of −120 mV and higher with increments of +20 mV and step intervals of 2 sec. **D**: I–V curve corresponding to parts A (solid line) and B (dotted line).

RESULTS

Voltage-clamp measurements on single isolated NRK cells and small cell clusters were performed to identify and characterize the ionic membrane conductances exhibited by these cells. In addition, excitability of NRK cells was studied by applying current-injections in single cells and cell clusters and by evoking propagating action potentials in monolayers.

Voltage-clamp measurements on single NRK cells

For the characterization of the membrane conductances in NRK cells, we first performed voltage-clamp experiments on isolated NRK cells that had been dissociated from quiescent confluent monolayers.

Under our standard conditions of voltage-clamp measurements (DF-ECS in the bath and S-ICS in the pipette), two types of voltage-dependent conductances were recognized as main conductances in single NRK cells, dissociated from quiescent monolayers (Fig. 1A): an inwardly rectifying potassium conductance (G_{Kir}) and an L-type calcium conductance (G_{CaL}). Consistent with its known properties (Hille, 2001), the inward rectifier was activated (actually unblocked from intracellular cations) upon hyperpolarization of the membrane to around and below its reversal potential and this reversal potential changed as expected for the equilibrium potential for K^+ ions when extracellular [K^+] was changed (n = 11). The inward rectifier was completely blocked by 1–5 mM external Ba^{2+} ions (n = 12) and the L-type calcium current was increased if Ba^{2+} instead of Ca^{2+} ions were used as charge carriers (Fig. 1B). The inward rectifier could also be blocked by 5–10 mM external Cs^+ ions (n = 4).

The presence of L-type currents in NRK fibroblasts had already been shown before in experiments on single NRK fibroblasts but in those experiments Ba^{2+} ions were used as charge carriers in order to increase the current for better resolution (De Roos et al., 1997c). Here we confirm the presence of this current for the more physiological condition that Ca^{2+} ions serve as charge carriers at approximately normal extracellular [Ca^{2+}] (2 mM). Under these conditions, the currents are smaller and have faster inactivation kinetics (Hille, 2001) (cf. Fig. 1A,B).

Besides G_{Kir} and G_{CaL}, we measured a calcium-activated chloride conductance $G_{Cl(Ca)}$ (further evidence is given below), which was very small using our standard strongly calcium buffering pipette solutions (Fig. 1A), but much larger using weakly buffering pipette solutions (Fig. 1C). Furthermore, it should be noted that I_{Kir} and I_{CaL} and $I_{Cl(Ca)}$ were usually superimposed on a leak current I_{leak}, conducted by a leak conductance (G_{leak}) which is the sum of the basal membrane leak conductance and the seal conductance.

Figure 1D shows the I–V curves corresponding to voltage-clamp measurements in parts A (solid lines) and B (dotted lines) for both total membrane currents at t = 500 msec and inward L-type current which was maximal at ~50 msec. These curves clearly demonstrate activation of G_{Kir} at hyperpolarized potentials (−120 and −100 mV) and inhibition of this conductance by Ba^{2+}. In addition, G_{CaL} was increased when calcium ions

TABLE 1. Calculated maximal conductances per cell in single normal rat kidney (NRK) cells and small clusters

	Condition	Single cells	Cell clusters
$G_{CaL,max}$	$[Ca^{2+}]_e = 2$ mM	0.67 ± 0.14 nS (n = 13)[d]	0.48 ± 0.08 nS (n = 23)[a,d]
	$[Sr^{2+}]_e = 2$ mM	N.D.[c]	0.98 ± 0.10 nS (n = 7)[b]
$G_{Cl(Ca),max}$	$[EGTA]_i = 3.5$ mM	0.14 ± 0.09 nS (n = 13)	0.47 ± 0.08 nS (n = 23)[a]
	$[EGTA]_i = 100$ μM	9.18 ± 1.61 nS (n = 17)	N.D.[c]
$G_{Kir,max}$		2.14 ± 0.46 nS (n = 13)	1.04 ± 0.13 nS (n=23)[a]
G_{leak}		0.29 ± 0.06 nS (n = 13)	0.10 ± 0.02 nS (n = 23)[a]

The maximal L-type calcium conductance ($G_{CaL,max}$) was calculated at its reversal potential (+50 mV), maximal calcium-activated chloride conductance ($G_{Cl(Ca),max}$) at +40 mV and maximal inwardly rectifying potassium conductance ($G_{Kir,max}$) at −120 mV. The leak conductance (G_{leak}) was calculated from the current at −80 mV, where $I_{Kir} = 0$ and assuming that $E_{leak} = 0$ mV. These four conductances were measured in the presence of extracellular calcium ($[Ca^{2+}]_e = 2$ mM) using standard intracellular calcium buffering (3.5 mM EGTA). In addition, $G_{CaL,max}$ was calculated under conditions that extracellular calcium was substituted by strontium ($[Sr^{2+}]_e = 2$ mM and $G_{Cl(Ca),max}$ under conditions that weak intracellular calcium buffering pipette solutions (100 μM EGTA) were used. Conductance values of the clusters were normalized by dividing by the number of cells in the cluster.
[a]Mean cluster size 5.6 ± 0.5 cells (n = 23).
[b]Mean cluster size 4.7 ± 0.6 cells (n = 7).
[c]Not determined.
[d]Not significantly different.

were replaced by barium ions. Based on the I–V curves maximal conductances of G_{CaL}, $G_{Cl(Ca)}$, G_{Kir}, and G_{leak} were calculated as described in Materials and Methods. Table 1 shows that $G_{Cl(Ca),max}$ is the smallest conductance (~0.14 nS) at strong intracellular calcium buffering, but the largest (~9.18 nS) at weak buffering. Furthermore, $G_{Kir,max}$ (~2.14 nS) > $G_{CaL,max}$ (~0.67 nS) > G_{leak} (~0.29 nS). In conclusion, voltage-clamp experiments on isolated NRK cells showed the presence of G_{CaL}, $G_{Cl(Ca)}$, and G_{Kir} as the main conductances in NRK cells.

Voltage-clamp measurements on clusters of NRK cells

In order to increase current amplitudes and to average for differences in conductances between individual cells, we explored the voltage-clamp properties of small clusters of NRK cells (two to ten cells), which are known to be electrically well coupled (De Roos et al., 1996).

The current amplitudes measured in clusters were increased compared to those in single cells (compare current scales in Figs. 1 and 2) but were similar to those in single cells when normalized for the number of cells in the cluster (see Table 1). For example, $G_{CaL,max}$ of single cells was not significantly different from that of cluster cells. This is consistent with acceptable voltage-clamp conditions for measuring these small calcium currents in cell clusters. By substitution of extracellular Ca^{2+} with Sr^{2+} ions the L-type current showed an increased amplitude and decelerated inactivation (Fig. 2B). The difference between $G_{Kir,max}$ for single cells and cluster cells may be due to non-ideal voltage-clamp conditions in clusters for the larger Kir currents (see Materials and Methods), although differences in cytoplasmic conditions between single cells and clusters may be another reason. Whereas the basal membrane conductance is proportional to the number of cells, the seal conductance is only determined by the leak between the patch pipette and the patched cell. Therefore, the leak conductance per cluster cell (G_{leak}) decreased with an increasing cluster size, becoming closer to the real membrane leak conductance per cell (~0.10 nS, see Table 1).

The delayed outward current through $G_{Cl(Ca)}$ was more easily studied in clusters (Fig. 2C), although the larger currents must have caused non-ideal voltage-clamp. $G_{Cl(Ca)}$ could be blocked by 50 μM BAPTA-AM (n = 3), which is a membrane permeable intracellular calcium buffer (Fig. 2D). In addition, this outward current disappeared after blocking G_{CaL} with 1 μM

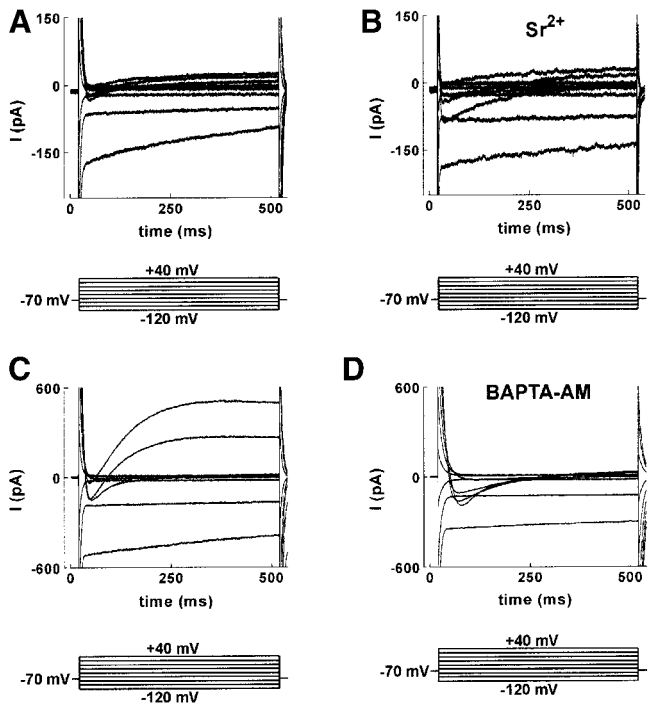

Fig. 2. Whole-cell current records in cell clusters. **A**: Cluster (four cells) with $G_{Kir,max} = 0.88$ nS, $G_{CaL,max} = 0.33$ nS, and $G_{Cl(Ca),max} = 0.09$ nS per cell, in the presence of 2 mM external Ca^{2+}. **B**: Same cluster (four cells) in the presence of 2 mM external Sr^{2+}. **C**: Cluster (ten cells) with $G_{Kir,max} = 1.19$ nS, $G_{CaL,max} = 0.61$ nS, and $G_{Cl(Ca),max} = 1.19$ nS per cell. **D**: Same cluster (ten cells) after 4 min perfusion with 50 μM BAPTA-AM. In all experiments, voltage-clamp steps were applied from a Vh of −70 mV to test potentials of −120 mV and higher with increments of +20 mV and step intervals of 2 sec.

nifedipine (n = 3) and was reversed to an inward current in the presence of a low (7.6 mM) external chloride concentration (n = 3). Apparently, Ca^{2+} ions that had entered the cells through L-type channels subsequently activated calcium-dependent chloride channels. Evidence for the existence of $G_{Cl(Ca)}$ in NRK fibroblasts has been shown before in current-clamp experiments on monolayers (De Roos et al., 1997a). Figure 2B shows that $G_{Cl(Ca)}$ could also be activated under conditions that external Ca^{2+} ions were substituted by Sr^{2+} ions. As a matter of fact, activation of $G_{Cl(Ca)}$ by Sr^{2+} ions has also already been shown before in voltage-clamp experiments on neurones (Akasu et al., 1990).

These results show that voltage-clamp experiments on small clusters of electrically coupled NRK cells allow the characterization of membrane conductances with better resolution (I_{CaL}) and under more physiological conditions ($I_{Cl(Ca)}$) than in single cells, due to increased current amplitudes and a reduced washout of cluster cells with pipette solution. Apparently, the coupling between the cells in a cluster is good enough (<10 MΩ, see Harks et al., 2001) to monitor voltage-clamp currents <50 pA. Larger currents may only give a qualitative impression of the properties of the measured conductances.

Characterization of the L-type current

In order to obtain more information about the kinetic properties of L-type calcium channels in NRK cells, we performed voltage-clamp experiments under conditions that $G_{Cl(Ca)}$ and G_{Kir} were absent. $G_{Cl(Ca)}$ was blocked by 50 μM NPPB and G_{Kir} and any other possible K^+ current was blocked by substituting K^+ for Cs^+ in the intracellular and for TEA^+ in the extracellular solution.

First, we tried to measure L-type currents in single NRK cells using the same voltage protocols as in Figures 1 and 2. However, the size of these currents (with Sr-ECS and Cs-ICS) was too small to do a reliable analysis, consistent with a current reducing effect of NPPB on I_{CaL} (Doughty et al., 1998). To improve the current resolution, we continued with experiments on small clusters of five to seven cells thereby using Sr^{2+} as the charge carrier to increase the current amplitude (cf. Fig. 2A,B). Figure 3A shows an example, in which the activation properties of G_{CaL} were determined in a cluster of six cells by applying increasing stepwise depolarizations of 750 msec duration from a holding potential (Vh) of −80 mV (Fig. 3A). Inward currents were evoked by steps to greater than −40 mV and were maximal at ~0 mV. All inward currents inactivated with

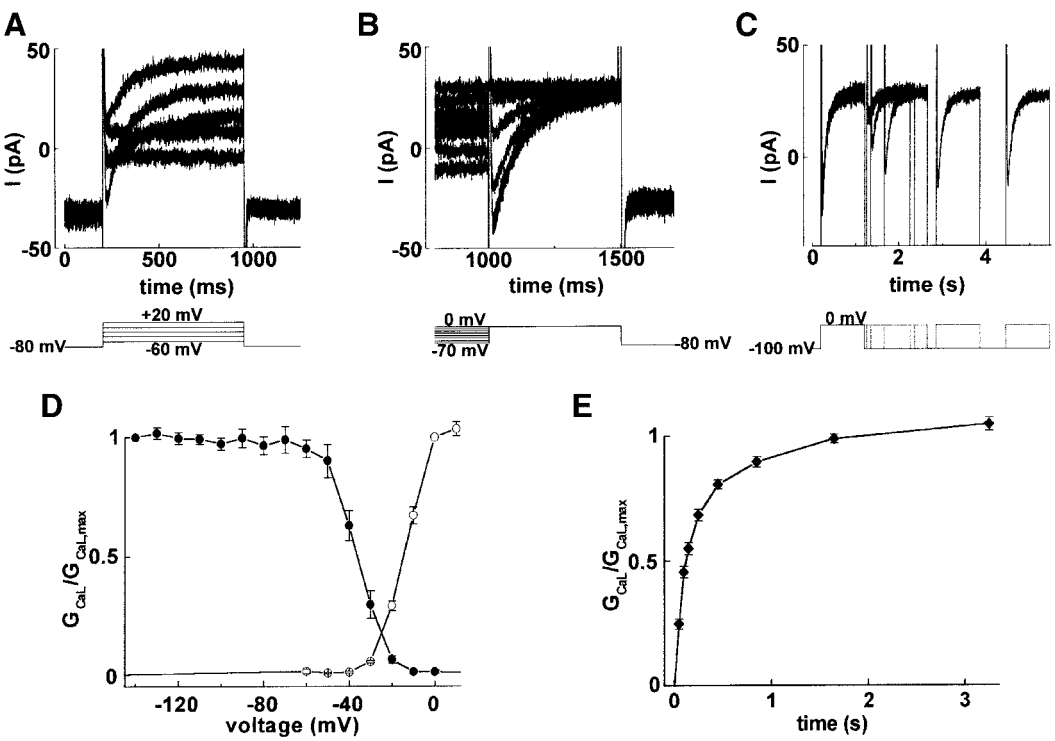

Fig. 3. Kinetic properties of the L-type current. **A**: Activation: in a cluster of six cells voltage-clamp steps were applied from a Vh of −80 mV to test potentials of −60 mV and higher with increments of +10 mV and sweep intervals of 2 sec. Voltage-steps of 750 msec to −60, −40, −20, 0, and +20 mV are shown. **B**: Inactivation: voltage-clamp steps were applied to the same cluster as in (A) from a Vh of −80 mV to (pre)potentials of −140 mV and higher with increments of +10 mV (prepulse duration 1 sec). Voltage-steps of 500 msec from prepulses of −70 mV and higher are shown. Each prepulse was followed by a test voltage-step to 0 mV and a step interval of 2 sec was used. **C**: Deinactivation: two consecutive voltage pulses were applied from a Vh of −100 mV to 0 mV (duration 1 sec) with increasing interpulse intervals (50, 100, 150, 250, 450, 850, 1,650, and 3,250 msec), while the sweep interval was 2 sec. Currents corresponding to interpulse intervals of 50, 150, 450, 1,650, and 3,250 msec are shown. **D**: Activation (-○-), inactivation (-●-), and (**E**) inactivation recovery (deinactivation) curve of the L-type current based on the currents measured in small clusters (mean ± SEM; n = 7) using voltage protocols as in parts A–C. Hundred percent activation in the activation and inactivation curve of $G_{CaL,max}$ corresponded to, respectively, 0.30 ± 0.02 and 0.33 ± 0.03 nS (n = 7). In all experiments 2 mM Sr^{2+} was used as charge carrier and $G_{Cl(Ca),max}$ and $G_{Kir,max}$ were blocked.

a time constant of ~200 msec towards leak current levels. In the same cluster, inactivation properties could be determined by measuring the leak-corrected maximal inward current at 0 mV, following a pre-potential of 1 sec duration and variable height (Fig. 3B). I_{CaL} was clearly reduced after pre-pulses of −50 mV and higher, indicating that this current inactivated at these potentials. Finally, deinactivation of G_{CaL} (at −100 mV) was measured by applying two consecutive voltage-steps to 0 mV from a Vh of −100 mV, whereby the interpulse interval was increasing (Fig. 3C). I_{CaL} gradually recovered upon increasing pulse-intervals.

Based on the currents measured in seven clusters of NRK cells, we could plot mean activation, inactivation, and deinactivation curves for G_{CaL}. Figure 3D shows that activation of G_{CaL} starts between −40 and −30 mV and is maximal at 0 mV. Mean half-maximal activation was determined from the individual activation curves and occurs at $E_{1/2a} = -14.3 \pm 0.8$ mV ($n = 7$). Inactivation starts at approximately −50 mV and is complete at 0 mV, while mean half-maximal inactivation was at $E_{1/2i} = -36.6 \pm 1.5$ mV ($n = 7$). Between −40 and −10 mV the activation and inactivation curves of G_{CaL} overlap, which could give rise to a small stationary calcium current around −20mV. Figure 3E shows that 50% deinactivation of G_{CaL} is achieved within ~124.6 ± 11.4 msec, while complete deinactivation is reached after ~2 sec.

Excitability of single NRK cells

We studied the electrophysiological properties of NRK cells by inducing action potentials in single cells in the presence of 2-mM external Sr^{2+}. Because of the variability of the resting membrane potential in these cells (De Roos, 1997), the excitability conditions of the cells were standardized by setting the membrane potential by a holding current at a standard value of ~80 mV.

First we tried to evoke an action potential in a single isolated NRK cell. Subthreshold depolarizations had time constants RmCm of the order of 60 msec, consistent with Cm ~20 pF and Rm ~3 GΩ (G_{leak} ~0.3 nS, see Table 1). Time constants increased with larger depolarizations because of closure of inward rectifier channels and decreased with hyperpolarization because of opening of these channels (see an illustration of this effect in Figure 5 for cluster stimulation, described below). By applying sufficiently strong positive current pulses in single cells, the membrane potential was depolarized beyond a certain threshold resulting in an action potential in seven of 25 cells tested. When the action potential was evoked using a strong intracellular calcium buffering solution, hardly any plateau phase of the action potential was measured (Fig. 4A). The contribution of $G_{Cl(Ca)}$ in the plateau phase became visible by reducing the calcium buffering capacity of the pipette solution ($n = 4$; Fig. 4B). The plateau phase of the action potential was markedly prolonged when intracellular calcium was weakly buffered, which confirms the calcium dependence of this conductance.

These results clearly demonstrate that electrical coupling is not required for excitability in a fraction of cells (~25%) since those single isolated NRK cells could fire action potentials. The inability of the non-responding cells could be due to a too small maximal G_{CaL} or due to a large G_{leak} and/or small seal resistance.

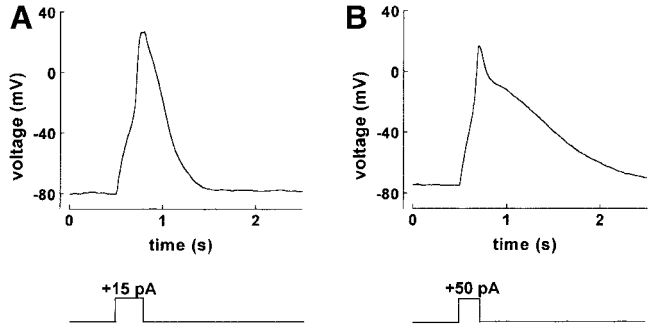

Fig. 4. Action potentials evoked in single NRK cells, in which the membrane potential was hold at a standard resting membrane potential of −80 mV by applying a negative holding current. **A**: Action potential evoked in a single cell ($G_{Kir,max} = 0.93$ nS, $G_{CaL,max} = 0.64$ nS, and $G_{Cl(Ca),max} = 0.98$ nS) with standard calcium buffering conditions by a current pulse of +15 pA. **B**: Action potential evoked in a single cell ($G_{Kir,max} = 2.18$ nS, $G_{CaL,max} = 5.19$ nS, and $G_{Cl(Ca),max} = 11.13$ nS) with low calcium buffering capacity ([EGTA] = 100 μM) by a current pulse of +50 pA. All experiments were performed with 2 mM external Sr^{2+}.

Excitability of clusters of NRK cells

In order to establish the involvement of electrical coupling in excitability of NRK cells, we performed current injections on small cell clusters of these cells, again in the presence of 2-mM external Sr^{2+}. The current pulses were applied to the patched cell, but due to the electrical coupling, the membrane potential response of the entire cluster (≤10 cells) was measured ($n = 23$). A negative holding current was used to establish a standard resting membrane potential of −80 mV. Some of the clusters ($n = 8$) had resting membrane potentials approximately −70 mV and were also excitable at that physiological membrane potential (i.e., without holding current).

All tested clusters were able to fire action potentials upon current stimulation. Typical membrane potential responses after current injections in a cluster of six cells are shown in Figure 5. In part A, the role of activation of G_{Kir} in the membrane potential response is clearly observed when a negative current pulse is applied. Under these conditions, the membrane hyperpolarizes, resulting in an activation of G_{Kir} and influx of K^+ ions into the cells, thereby counteracting the hyperpolarization. This part also demonstrates the upstroke of the action potential upon activation of G_{CaL} around −35 mV, the approximate threshold potential for activation of G_{CaL}. Figure 5B shows the response of the same cluster upon two consecutive current pulses with increasing interpulse intervals. After repolarization of the first action potential, the cells are capable of firing a second action potential within 1 sec, consistent with the time course of the deinactivation of G_{CaL} shown in Figure 3E. Figure 5C shows typical action potentials evoked in a cluster of six cells, which had a more than five times smaller $G_{Kir,max}$:$G_{Cl(Ca),max}$ ratio, while G_{CaL} was similar. In this cluster, action potentials could already be evoked by application of a smaller current pulse (+40 pA compared to +60 pA in part A), while the duration of the

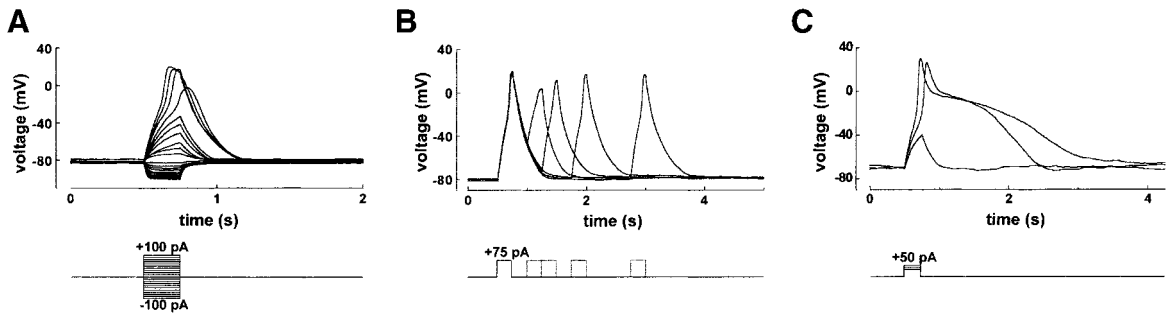

Fig. 5. Action potentials evoked in small clusters of NRK cells. The resting membrane potential was kept at −80 mV by a negative holding current. **A**: Membrane potential response of a cluster of six cells ($G_{Kir,max} = 1.59$ nS, $G_{CaL,max} = 0.94$ nS, and $G_{Cl(Ca),max} = 3.00$ nS per cell) upon application of current pulses with an amplitude ranging from −100 pA to +100 pA with step intervals of +10 pA. **B**: Action potentials evoked in the same cluster. In each sweep two consecutive action potentials were evoked by current pulses of +75 pA and the interpulse interval was doubled in every following sweep (250, 500, 1,000, and 2,000, and 4,000 msec). The time between two successive double-pulse sweeps was 2 sec. **C**: Membrane potential response of another cluster of six cells ($G_{Kir,max} = 0.17$ nS, $G_{CaL,max} = 0.85$ nS, and $G_{Cl(Ca),max} = 1.80$ nS per cell) upon application of current pulses of +30, +40, and +50 pA. All experiments were performed with 2 mM external Sr^{2+}.

plateau phase was much longer. In general, the duration of the plateau phase seemed to correlate with the relative size of the conductances present in clusters of five to eight cells, such that the time required for 50% repolarization of the action potential was significantly longer in clusters with smaller G_{Kir}:$G_{Cl(Ca)}$ ratios ($0.025 > P > 0.01$; n = 13). The correlation with both conductances alone also exists, but is less significant ($0.1 < P < 0.05$; n = 13).

Excitability of confluent NRK monolayers

Previously we have shown that it is possible to evoke propagating action potentials in confluent monolayers of NRK cells (De Roos et al., 1997b), and here we further explored the contribution of the membrane conductances identified in this study to the shape of this action potential by specifically blocking one of the conductances.

With the equipment available, it was not possible to inject sufficient current into one cell of the monolayer to evoke an action potential due to the low input resistance of the monolayer because of gap junctional coupling between the cells. However, monolayers can be excited by a depolarization of cells in a small area by either a local elevation of extracellular [K^+] or by the local application of an intracellular calcium mobilizing agent (e.g., bradykinin) (De Roos et al., 1997b). These action potentials were measured in only about 10% of the monolayer cultures using normal Ca^{2+} containing media, but the incidence was increased to almost 100% when Ca^{2+} was replaced by Sr^{2+}. Therefore, we also substituted external Ca^{2+} by Sr^{2+} ions. A typical example of an action potential evoked by a high extracellular [K^+] stimulus under these conditions is shown in Figure 6A. The duration of the action potential evoked in monolayers is much more prolonged (∼30 sec) compared to that evoked in single cells (∼2 sec; Fig. 4B) and small cell clusters (∼3 sec; Fig. 5C).

When G_{CaL} was completely blocked by nifedipine (1 μM), it was not possible to evoke an action potential (Fig. 6B, n = 4), which is in accordance with earlier results of De Roos et al. (1997b).

Activation of $G_{Cl(Ca)}$ could be prevented by buffering intracellular calcium upon application of BAPTA-AM (50 μM). Under these conditions, a propagating action potential could still be evoked but the plateau phase of the action potential was completely abolished (Fig. 6C, n = 4), indicating that a rise in the intracellular calcium concentration is required for activation of the chloride conductance that accounts for the prolonged plateau phase of the action potential. The remaining shortened action potential is wider than the initial spike of the normal action potential. This implies that $G_{Cl(Ca)}$ normally contributes to the repolarization of the initial Ca^{2+} or Sr^{2+} driven spike of the action potential.

The role of G_{Kir} in the electrical behavior of the cells was assessed by blocking G_{Kir} with Cs^+ ions (10 mM). After addition of Cs^+, the membrane immediately started to depolarize to about −50 mV (n = 5), which indicates that G_{Kir} is important for setting the resting membrane potential around −70 mV. When a propagating action potential was evoked under conditions that G_{Kir} was blocked, the action potential exhibited a prolonged plateau phase (n = 5) or did not repolarize at all (n = 2). Figure 6D shows the effect of blocking G_{Kir} on the membrane potential of a monolayer of NRK cells and the prolonged plateau phase of the evoked action potential. In this particular example, after 4 min, the action potential only partially repolarized to −40 mV. As a consequence the cells became competent to spontaneously fire a second action potential that did not repolarize within the time of observation (>20 min).

In conclusion, the action potential evoked in NRK monolayers clearly results from a sequential opening of G_{CaL}, $G_{Cl(Ca)}$, and G_{Kir}, respectively.

DISCUSSION

In the present study, we have characterized three principal membrane conductances in NRK fibroblasts by whole-cell voltage-clamp experiments and we have shown how excitability of the cell results from an interplay between these conductances via the membrane potential and intracellular calcium. These conductances are an inwardly rectifying potassium conductance (G_{Kir}), an L-type calcium conductance (G_{CaL}) and a calcium-activated chloride conductance ($G_{Cl(Ca)}$). Unique for this action potential is that the intracellular calcium dynamics is an essential part of the excitability

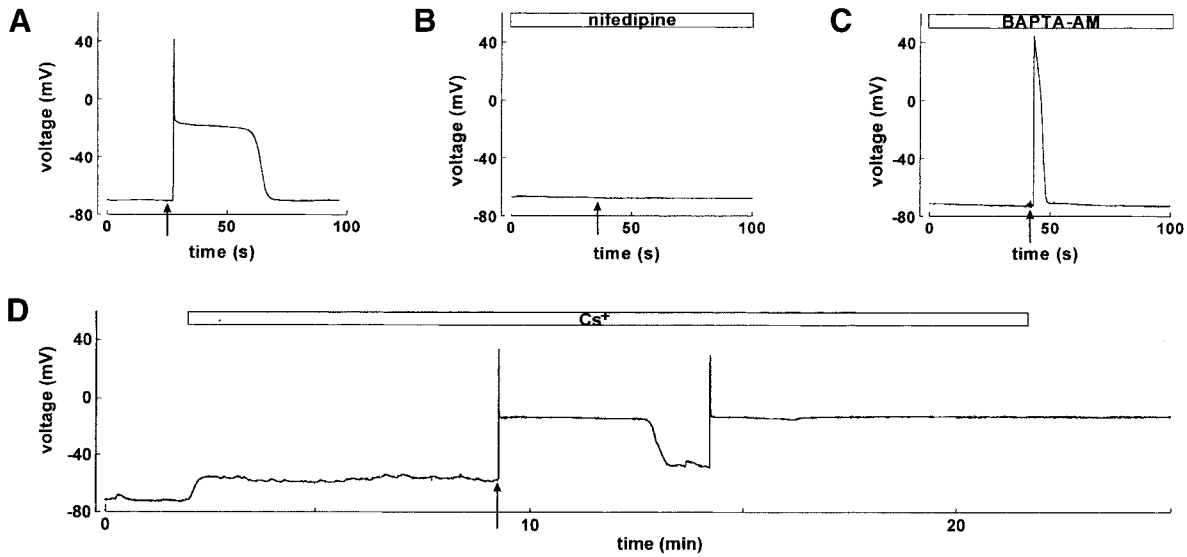

Fig. 6. Contribution of membrane conductances to action potentials evoked in an NRK monolayer. Action potentials were evoked in a confluent monolayer by one distant stimulation (indicated by the arrow) of a few cells with a small volume (10 μl) of 124 mM KCl under conditions that: (**A**) control (**B**) G_{CaL} was blocked by 1 μM nifedipine, (**C**) $G_{Cl(Ca)}$ was blocked by preincubation (10 min) with 50 μM BAPTA-AM and (**D**) G_{Kir} was kept inactive by 10 mM Cs^+. All experiments were performed with 2 mM external Sr^{2+}.

mechanism. Thus, both voltage-dependent (G_{CaL}, G_{Kir}) and calcium-dependent ($G_{Cl(Ca)}$) properties of the conductances involved essentially contribute to excitability.

Although fibroblasts are often considered as non-excitable cells, we have previously shown that in quiescent monolayers of NRK cells, which have a stable resting potential around −70 mV, a propagating action potential can be triggered that propagates throughout the entire monolayer (De Roos et al., 1997b). Such an action potential is induced by a depolarization of the membrane beyond the threshold for activation of G_{CaL} and the incidence of action potentials was increased from only about 10% in Ca^{2+} containing medium to almost 100% when external Ca^{2+} was replaced by Sr^{2+} ions. Voltage-clamp experiments now show that under these conditions G_{CaL} was about twofold increased whereas inactivation of this conductance was also slower.

The action potentials evoked in monolayers of NRK cells are characterized by a typical long-duration (~30 sec) plateau phase. This plateau results from activation of $G_{Cl(Ca)}$ after Ca^{2+} or Sr^{2+} entry through L-type calcium channels and disappeared when these divalent ions were buffered using BAPTA-AM. The dependence of activation of this chloride conductance on calcium entry through L-type calcium channels was confirmed by voltage-clamp experiments. Membrane current recordings of cell clusters showed that BAPTA-AM did not block the inward calcium current, whereas the outward calcium-activated chloride current was completely abolished. In addition, voltage-clamp experiments on single cells showed that under our standard (strong) calcium buffering conditions (i.e., 3.5 mM EGTA in internal pipette solution) hardly any outward chloride current was measured, and that the action potential evoked by a current pulse did not have a plateau phase. However, when measured with weak calcium buffering pipette solutions (100 μM EGTA) this current was largely increased and the action potential showed a prominent plateau phase. These results clearly demonstrate that $G_{Cl(Ca)}$ generates the plateau phase of the action potential. In addition, activation of the $G_{Cl(Ca)}$ by the rise in cytoplasmic $[Ca^{2+}]$ following the inflow of calcium or strontium through the G_{CaL} channels and probably supported by release of calcium from internal stores contributes to the repolarization of the initial spike of the action potential. This initial repolarization occurs at voltages of 0 to +40 mV, where the G_{Kir} channels are expected to be fully inactive. However, outward rectification of $G_{Cl(Ca)}$ may also contribute to that initial repolarization mechanism.

So far, only the presence of G_{CaL} and $G_{Cl(Ca)}$ has been reported for NRK fibroblasts (De Roos et al., 1997a,c). Here we show for the first time, that NRK fibroblasts also express a G_{Kir}. Expression of inwardly rectifying potassium channels has been shown before in fibroblasts such as human dermal fibroblasts (Estacion, 1991), but their function has remained elusive. In NRK fibroblasts, G_{Kir} appears to be essential for the generation of the resting membrane potential as blocking this conductance with Cs^+ ions depolarized the cells from around −70 to −50 mV. Under these conditions, an action potential could still be evoked but the repolarization of the action potential was impaired. Previously it has been shown that the action potentials in NRK cells are accompanied by intracellular calcium transients, and it was suggested that repolarization of the action potential occurred concomitant to the return of intracellular calcium concentrations to basal levels (De Roos et al., 1997b,c). Although this decrease in intracellular calcium levels indeed would shut off $G_{Cl(Ca),max}$, we now know that it is insufficient to completely repolarize the

cells to resting values of the membrane potential around −70 mV. The closure of the chloride channels, namely, will make the membrane subject to the repolarizing effect of I_{Kir}, which is required for the complete repolarization of the cells. This is in agreement with the results in Figure 5C where a significantly prolonged plateau phase of the action potential was measured in a cluster with a relatively small $G_{Kir,max}$:$G_{Cl(Ca),max}$ ratio. Moreover, blocking the activation of G_{Kir} with Cs^+ prevented a complete repolarization of the action potential. These results demonstrate that activation of G_{Kir} is essential for the complete repolarization of the action potential to the resting value of the membrane potential around −70 mV. This finding is in agreement with recently published data, showing that G_{Kir} is activated around −20 mV and constitutes one of the major components for the repolarization of the cardiac action potential from −20 to −60 mV (Ishihara et al., 2002). We have never found evidence for another repolarizing conductance with a reversal potential E_{rev} rather more negative than −20 mV. Any chloride conductance G_{Cl} will have an E_{rev} approximately −20 mV, thus will be unable to contribute to the final repolarization. Any leak detected reverses around 0 mV (cf. Fig. 1D) and we never detected a delayed rectifier type of K^+ conductance. So, the only repolarizing conductance seems to be G_{Kir}. The fact that the leakage conductance G_{leak} (per cell) of gap junctionally coupled cells in cell clusters is relatively small (approximately <0.1 nS, see Table 1) implies that the repolarizing conductance needs to be very small, since $G_{Cl(Ca)}$ is declining to very low values due to calcium sequestering during the AP plateau. Thus, an extra G_{leak} or background conductance is probably not required for AP repolarization. Nevertheless, a very small background potassium conductance other than G_{Kir} cannot be excluded and a role for electrogenic ion transporters such as the Na/K-pump also remains a possibility. However, because we have been able to generate NRK-cell resting membrane potentials and action potentials with a mathematical model that only includes G_{Kir}, G_{CaL}, $G_{Cl(Ca)}$, and a small aselective G_{leak} (Torres et al., 2003), we have reasons not to invoke other repolarizing conductances. The role of G_{Kir} in the repolarization results from reactivation of G_{Kir} after deactivation during the upstroke of the action potential. Thus, G_{kir} also plays a role in action potential depolarization and in maintaining the plateau phase, as in heart cells, because deactivation accelerates the initial depolarization and in the deactivated state G_{Kir} allows $G_{Cl(Ca)}$ to dominate the membrane potential in the plateau phase.

The present study also provided an initial characterization of the activation and inactivation properties of the NRK-cell L-type calcium conductance (Fig. 3), when it conducts Sr^{2+} ions. Although these properties should be checked for conditions where G_{CaL} is not reduced (here by NPPB, consistent with Doughty et al., 1998), they allow a first comparison with current-clamp properties of NRK-cells. The voltage-clamp experiments showed that the threshold for I_{CaL} activation is around −40 mV (see Fig. 3D) where inactivation is not far advanced (∼50%). This explains that monolayer cells could spontaneously fire a second action potential after partial repolarization of the membrane to around −40 mV under conditions that G_{Kir} was blocked by Cs^+ (Fig. 6D). This finding suggests that any means that would depolarize the cells towards this potential should render them competent to fire an action potential. Indeed, previously we measured that cells fired an action potential if they became progressively depolarized by slow superfusion with medium containing an increasing K^+ concentration (De Roos et al., 1997d).

Excitability of NRK fibroblasts has so far only been measured in confluent monolayers (De Roos et al., 1997b,c). Under those conditions, the cells are electrically well coupled by gap junctions and share each other's membrane conductances (Harks et al., 2001). However, electrical coupling appears not to be required for action potential firing since action potentials could be evoked in a significant percentage (∼25%) of the single isolated NRK cells. The duration of the plateau phase of the action potential was, however, much shorter in single cells and clusters of cells compared to those evoked in monolayers. One reason of this difference may be that the whole-cell conditions established by the measuring patch pipette disturb the intracellular calcium dynamics in single cells and small cell clusters even with weak calcium buffering pipette solutions. In that case, the activation of $G_{Cl(Ca)}$ channels would become mainly dependent on inflow of calcium through G_{CaL} channels and would no longer be supported by calcium release from intracellular stores.

The resting membrane potential of dissociated NRK cells varied enormously between cells, with values ranging from −10 to −75 mV. This large variability is most likely caused by the variation in the seal resistances (1–10 GΩ). Although the estimated maximal values of G_{Kir} are relatively high at −120 mV, G_{Kir} at −70 mV (resting membrane potential in monolayers) is often smaller (cf. the slope of the I–V-curve around −70 mV in Fig. 1D) than the single cell leak conductance (∼0.3 nS). Therefore, the resting membrane potential in single cells is very sensitive to changes in the seal resistance. This variability in seal resistance may also explain why only a fraction of the single cells (∼25%) was excitable. However, variability in expression of G_{Kir} (for the resting membrane potential) and G_{CaL} channels (for excitability) may also underlie the differences in excitability of single cells. In cell clusters and monolayers, the leak conductance becomes much less effective in depolarizing the resting membrane potential, because the surrounding cells provide a relatively larger (summed) G_{Kir}. Moreover, the variability in the expression of G_{CaL} channels is sum-averaged over the whole cluster and the channels in the surrounding cells may be less subjected to run-down, because the intracellular milieu of those cells is screened off from the pipette-perfused cell by gap junctional channels. These effects together may explain why in contrast to single cells, all cell clusters were excitable.

The characterization of ionic membrane conductances was performed in cells derived from monolayers of quiescent NRK cells. When these monolayers are treated with epidermal growth factor (EGF) as the only growth stimulating polypeptide, the cells are induced to enter the cell division cycle and become arrested in their growth when they have reached a critical cell density

(van Zoelen, 1991). In contrast to their quiescent counterparts, which exhibit a stable resting membrane potential around −70 mV, the growth-arrested cells (also called density-arrested) have been shown to spontaneously fire calcium action potentials with an interspike interval of approximately 150 sec. The shape of these periodic action potentials is identical to that of the single action potential induced in quiescent monolayers and is also accompanied by transient increases in cytoplasmic calcium concentration (De Roos et al., 1997c). Preliminary voltage-clamp experiments on NRK cells derived from growth-arrested monolayers have shown that these cells express the same three prominent membrane conductances as their quiescent counterparts. Thus, spontaneous firing of density-arrested cells does not seem to result from the expression of extra ion channel types in the plasma membrane. Therefore, the mechanism providing the periodicity of the calcium spiking in density-arrested cells still remains unknown.

We now show by current injections in cell clusters that NRK cells are capable to fire a subsequent action potential within 1 sec after repolarization of a preceding action potential. This is in agreement with voltage-clamp data, which showed that G_{CaL} was largely (~85%) deinactivated within 1 sec (Fig. 3E). Obviously, the interspike interval in repetitively firing growth-arrested NRK monolayers (~150 sec) is not determined by a refractory period of the action potential due to inactivation of the calcium channels. In accordance with that notion, it was found that an additional action potential could be evoked between two spontaneously fired consecutive action potentials by local stimulation with a high external [K^+] pulse (De Roos et al., unpublished observation).

Possibly, the periodicity of spontaneous action potential firing by density-arrested NRK cells is determined by oscillatory changes in their intracellular calcium concentration. In recent years, three different types of intracellular calcium stores have been identified, which are the IP_3-sensitive, cADPR-sensitive and NAADP-sensitive calcium stores (see, e.g., Cancela et al., 2000). It has also been shown that a periodic release and uptake of calcium in one or more of these stores can result in intracellular calcium oscillations (see for review, e.g., Patel et al., 2001). We hypothesize that in density-arrested NRK monolayers such oscillatory intracellular calcium rises transiently activate $G_{Cl(Ca)}$ by which the cells depolarize beyond the threshold for activation of G_{CaL}, and thereby fire action potentials periodically. Our current research is aimed at resolving the role and interplay of the different calcium stores in the oscillatory behavior of NRK cells and to address the question why spontaneous oscillatory behavior is exhibited by density-arrested NRK fibroblasts and not by their quiescent counterparts.

In the present study, we have elucidated the ionic basis for excitability of cultured NRK fibroblasts, but we can still only speculate on the in vivo function of this excitability. As fibroblasts form cellular communicating networks in vivo (Komuro, 1989, 1990; Hashizume et al., 1992) which expand throughout entire organs, their excitability in combination with electrical coupling might provide them with an efficient tool for fast and long-distance intercellular signaling. In this way, agonist-induced depolarizations evoked in a few cells may be transduced to unstimulated neighboring cells, thereby recruiting a greater population of cells to respond in unison to local stimuli. As a matter of fact, we have found that action potentials induced in NRK fibroblasts can be transduced via heterocellular gap junctions to epithelial NRK cells, when both cell types are co-cultured (De Roos, 1997). This suggests that in vivo fibroblasts may couple to different cell types in a tissue and may act as an excitable and conductive pathway by which electrical signals generated at one side of a tissue or organ can be transduced to the other side. Also in other cells, the membrane potential has been shown to be involved in the coordination of cellular processes. For instance, calcium oscillations in pancreatic islets are synchronized by associated membrane potential changes (Santos et al., 1991). In addition, it has been shown that electrical coupling between endothelial cells and smooth muscle cells is implicated in the transmission of a hyperpolarization (Beny and Pacicca, 1994), presumably involved in vasoconstriction.

In conclusion, the results of the present study clearly demonstrate that a collection of only three types of ion channels besides leak channels, namely, G_{Kir}, G_{CaL}, and $G_{Cl(Ca)}$ channels, may be sufficient to provide single NRK cells with a mechanism for slow action potential generation. G_{Kir} and G_{CaL} are sufficient to produce conventional fast action potentials. Peculiar in the NRK cell excitability mechanism is the essential role of the intracellular calcium dynamics, coupling the activity of $G_{Cl(Ca)}$ channels to the activity of the depolarization activated G_{CaL} channels. Gap junctional coupling of cells does not only allow long-distance intercellular propagation of these action potentials, but also improves the excitability of neighboring cells with differences in channel expression by channel sharing.

ACKNOWLEDGMENTS

We thank Peter Peters for technical assistance in culturing NRK cells and Dr. W.P.M. Van Meerwijk for statistical advice. JJT acknowledges support from the Spanish Ministerio de Ciencia y Technologia and FEDER ("Ramón y Cajal" contract and contract grant number BFM2001-2841, and partial support from University of Granada (Plan Propio de Investigación) and Dutch Foundation for Neural Networks (SNN). DLY is supported by the Foundation Nijmegen University Fund (SNUF).

LITERATURE CITED

Akasu T, Nishimura T, Tokimasa T. 1990. Calcium-dependent chloride current in neurones of the rabbit pelvic parasympathetic ganglia. J Physiol 422:303–320.

Beny JL, Pacicca C. 1994. Bidirectional electrical communication between smooth muscle and endothelial cells in the pig coronary artery. Am J Physiol 266:H1465–H1472.

Cancela JM, Gerasimenko OV, Gerasimenko JV, Tepikin AV, Petersen OH. 2000. Two different but converging messenger pathways to intracellular Ca(2+) release: The roles of nicotinic acid adenine dinucleotide phosphate, cyclic ADP-ribose, and inositol trisphosphate. Embo J 19:2549–2557.

De Roos AD. 1997. PhD. Thesis. University of Nijmegen.

De Roos AD, van Zoelen EJ, Theuvenet AP. 1996. Determination of gap junctional intercellular communication by capacitance measurements. Pflugers Arch 431:556–563.

De Roos AD, Van Zoelen EJ, Theuvenet AP. 1997a. Membrane depolarization in NRK fibroblasts by bradykinin is mediated by a calcium-dependent chloride conductance. J Cell Physiol 170:166–173.

De Roos AD, Willems PH, van Zoelen EJ, Theuvenet AP. 1997b. Synchronized Ca^{2+} signaling by intercellular propagation of Ca^{2+} action potentials in NRK fibroblasts. Am J Physiol 273:C1900–C1907.

De Roos AD, Willems PH, Peters PH, van Zoelen EJ, Theuvenet AP. 1997c. Synchronized calcium spiking resulting from spontaneous calcium action potentials in monolayers of NRK fibroblasts. Cell Calcium 22:195–207.

De Roos AD, Van Zoelen EJ, Theuvenet AP. 1997d. Wirtz KW, editor. Molecular mechanisms of signalling and targeting. NATO ASI series. Springer Verlag. pp 113–126.

Doughty JM, Miller AL, Langton PD. 1998. Non-specificity of chloride channel blockers in rat cerebral arteries: Block of the L-type calcium channel. J Physiol 507:433–439.

Estacion M. 1991. Characterization of ion channels seen in subconfluent human dermal fibroblasts. J Physiol 436:579–601.

Harks EG, De Roos AD, Peters PH, de Haan LH, Brouwer A, Ypey DL, van Zoelen EJ, Theuvenet AP. 2001. Fenamates: A novel class of reversible gap junction blockers. J Pharmacol Exp Ther 298:1033–1041.

Hashizume T, Imayama S, Hori Y. 1992. Scanning electron microscopic study on dendritic cells and fibroblasts in connective tissue. J Electron Microsc (Tokyo) 41:434–437.

Hille B. 2001. Ion channels of excitable membranes. Sunderland, MA, USA: Sinauer Associates, Inc.

Ishihara K, Yan DH, Yamamoto S, Ehara T. 2002. Inward rectifier K^+ current under physiological cytoplasmic conditions in guinea-pig cardiac ventricular cells. J Physiol 540(Pt 3):831–841.

Komuro T. 1989. Three-dimensional observation of the fibroblast-like cells associated with the rat myenteric plexus, with special reference to the interstitial cells of Cajal. Cell Tissue Res 255:343–351.

Komuro T. 1990. Re-evaluation of fibroblasts and fibroblast-like cells. Anat Embryol (Berlin) 182:103–112.

Lahaye DH, Walboomers F, Peters PH, Theuvenet AP, Van Zoelen EJ. 1999. Phenotypic transformation of normal rat kidney fibroblasts by endothelin-1. Different mode of action from lysophosphatidic acid, bradykinin, and prostaglandin 2alpha. Biochim Biophys Acta 1449:107–118.

Patel S, Churchill GC, Galione A. 2001. Coordination of Ca^{2+} signalling by NAADP. Trends Biochem Sci 26:482–429.

Santos RM, Rosario LM, Nadal A, Garcia-Sancho J, Soria B, Valdeolmillos M. 1991. Widespread synchronous $[Ca^{2+}]_i$ oscillations due to bursting electrical activity in single pancreatic islets. Pflugers Arch 418:417–422.

Schoenmakers TJ, Visser GJ, Flik G, Theuvenet AP. 1992. CHELATOR: An improved method for computing metal ion concentrations in physiological solutions. Biotechniques 12:870–874.

Torres JJ, Cornelisse LN, Harks EGA, Theuvenet APR, Ypey DL. 2003. Modeling action potential (AP) generation and propagation in quiescent fibroblastic (NRK) Cells. Biophys J 84 , Number 2, Part 2 of 2 (Supplement), 393a, 1915-Pos, (abstract).

Van Zoelen EJ. 1991. Phenotypic transformation of normal rat kidney cells: A model for studying cellular alterations in oncogenesis. Crit Rev Oncog 2:311–333.